

# Communication between neocortex and hippocampus during sleep in rodents

Anton Sirota, Jozsef Csicsvari, Derek Buhl, and György Buzsáki\*

Center for Molecular and Behavioral Neuroscience, Rutgers, State University of New Jersey, 197 University Avenue, Newark, NJ 07102

Communicated by Jan Bureš, Czech Academy of Sciences, Prague, Czech Republic, December 27, 2002 (received for review December 5, 2002)

**Both neocortical and hippocampal networks organize the firing patterns of their neurons by prominent oscillations during sleep, but the functional role of these rhythms is not well understood. Here, we show a robust correlation of neuronal discharges between the somatosensory cortex and hippocampus on both slow and fine time scales in the mouse and rat. Neuronal bursts in deep cortical layers, associated with sleep spindles and delta waves/slow rhythm, effectively triggered hippocampal discharges related to fast (ripple) oscillations. We hypothesize that oscillation-mediated temporal links coordinate specific information transfer between neocortical and hippocampal cell assemblies. Such a neocortical–hippocampal interplay may be important for memory consolidation.**

The means by which ensembles of neurons interact with each other for an effective transfer and storage of information are not well understood. It is generally believed that network oscillatory rhythms within and across structures support these functions (1, 2). One current working hypothesis is that information transfer at the hippocampal–neocortical interface in sleep–wake cycle is involved in the encoding and consolidation of memories (3–12). The oscillatory patterns in these structures are fundamentally different in states of waking and sleep (13–15). Attentive, exploratory behavior is characterized by neocortical fast gamma activity and hippocampal theta/gamma oscillations (16–18). The most prominent hippocampal pattern during slow wave sleep is a transient burst of CA3–CA1 pyramidal cells associated with a sharp wave in stratum (str.) radiatum and fast field oscillation (140- to 200-Hz ripple) in the CA1 pyramidal layer (19–21). Sleep patterns of the neocortex include thalamocortical sleep spindles (12–18 Hz) and delta waves (1–4 Hz) (13, 22). Whether and how these macroscopic rhythms support the coding, transfer, and consolidation of information is not understood.

Recently, it has been suggested that hippocampal ripples and sleep spindles in the prefrontal cortex are temporally linked on the scale of  $\approx 1$  s (23). Whether neurons of the hippocampus and neocortex are involved in a more specific spatiotemporal interaction during sleep remains to be explored. To address this issue, we used multisite recording of unit and field activity in the hippocampus and somatosensory cortex. The somatosensory cortex was chosen because it is the most prominent source of sensory information in the rat (24), and, unlike the prefrontal cortex (25), it does not receive monosynaptic input from the hippocampus. Here, we demonstrate temporal coupling of neuronal activity between the somatosensory cortex and hippocampus on both slow and fine time scales and show that neocortical activity can time the occurrence of hippocampal sharp waves and ripples. Such coupling may assist linking neocortical and hippocampal cell assemblies during slow wave sleep.

## Materials and Methods

Ten male mice (six progeny of C57B6/J and 129S6/SvEvTac hybrid mice and four connexin36 knockout; ref. 26; 30–40 g) and four male Sprague–Dawley rats (300–400 g) were implanted with a microdrive that allowed the positioning of

recording electrodes in the somatosensory neocortex and/or the dorsal hippocampus. In mice, the electrodes were either single wires (60- $\mu$ m diameter) or “tetrodes” (27, 28). Four rats were equipped with single ( $n = 2$ ) or double ( $n = 2$ ) 16-site silicon probes (with recording sites at 100- $\mu$ m vertical spacing) for simultaneous recording of unit activity and field potentials in different cortical layers and hippocampus. The position of the electrodes was confirmed histologically. All procedures conformed to the National Institutes of Health Guide for the Care and Use of Laboratory Animals and had been approved by the Institutional Animal Care and Use Committee at Rutgers.

Recordings were carried out in the home cage while the animal was sleeping or immobile (1-Hz to 5-kHz frequency band; 20-kHz digitization rate). Data processing was done off-line. Units were isolated by a semiautomatic cluster analysis program, followed by manual adjustments using wave shape and cross/autocorrelogram information (27, 29). Local field potentials were filtered for a particular frequency range by using continuous wavelet transformation (30). Peaks of neocortical delta waves and troughs of sleep spindles and hippocampal ripples were detected as maxima/minima of filtered signal that corresponded to larger than 3 SD of the instantaneous log-power in the same frequency band. In the case of delta waves, recorded in deep layers (V–VI), detection of peaks was more reliable than detection of troughs; therefore, peaks were used for quantitative analyses. Spike–spike, spike–wave, and wave–wave time correlations were assessed by cross-correlograms. Cross-correlograms were normalized by the asymptotic mean firing rates of both trains to obtain correlation index (c.i.). A c.i. of 1 corresponds to independent firing, and a c.i.  $>1$  indicates correlated firing. To investigate the temporal relationship between unit firing in neocortex and hippocampus and times of peaks of network oscillations, we used joint probability density of the lags between unit firing in the two structures from the time of oscillation peaks (31).

In rats, current source density (CSD) analysis (32) of the simultaneously recorded field potentials was used to eliminate volume conduction and localize actual depth of synaptic currents. Space was assumed isotropic, and changes of resistivity across layers were neglected. A 2D matrix of potentials in space/time was transformed into a CSD signal (33), using a spatial differentiation scheme, that effectively smoothed spatial noise. Spectral analyses were carried out by direct multitaper estimates (34, 35) using five to nine tapers. Event-triggered spectrograms were computed from electroencephalogram segments of 60 s centered on hippocampal ripples peak, normalized by the mean spectrum over the entire session and then log-transformed for visualization purposes (as shown in Fig. 1*b*). To investigate the temporal relationship between hippocampal ripples and neocortical delta and spindle events on a slow time scale, cross-correlation between the respective powers was computed in the following manner. Spectral power

Abbreviations: CSD, current source density; c.i., correlation index.

\*To whom correspondence should be addressed. E-mail: buzszaki@axon.rutgers.edu.

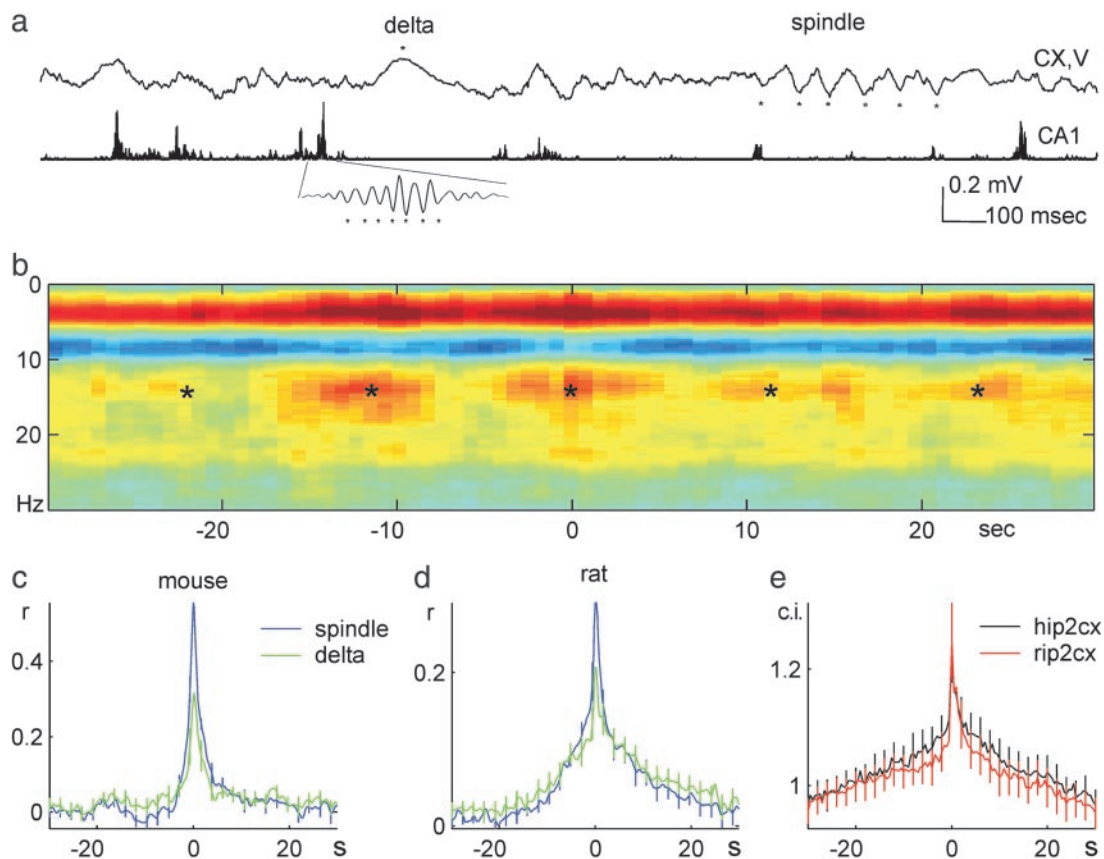


**Fig. 1.** Slow time scale correlation between neocortical and hippocampal patterns during slow wave sleep. (a) Traces of neocortical layer V (1 Hz–3 kHz) and hippocampal CA1 (filtered between 140 and 240 Hz and rectified) electroencephalogram in a rat. (Inset) Filtered ripple at a faster time scale. \*, Peak of delta and troughs of sleep spindle and hippocampal ripple. Positive polarity is up in this and subsequent figures. (b) Hippocampal ripple-triggered neocortical spectrogram in a mouse. Powerspectrograms, centered on ripples (time 0 s;  $n = 147$ ), were averaged and normalized by the mean power over the entire recording session and log transformed. Note increased correlation of power in the delta (1–4 Hz) and sleep spindle (10–18 Hz) bands with hippocampal ripples. \*, Slow ( $\approx 0.1$  Hz) comodulation of neocortical and hippocampal activity. The magnitude and frequency of slow comodulation (0.03–0.3 Hz) varied from animal to animal. (c and d) Group averages of cross-correlograms of ripple power (time 0 s) to spindle and delta power (blue and green lines, respectively) in mice (c,  $n = 10$ ) and rats (d,  $n = 4$ ). (e) Hippocampal ripple vs. deep layer neocortical unit cross-correlogram (rip2cx) and hippocampal CA1 unit vs. neocortical unit cross-correlogram (hip2cx;  $n = 10$  mice).

in these frequency bands was calculated in overlapping 1-s windows, providing a time series, which were log-transformed and cross-correlated.

## Results

**Slow Time Scale Analysis.** The relationship between hippocampal and neocortical local field and unit activity was studied in freely moving mice and rats during periods of immobility and slow wave sleep (Fig. 1a). To determine which neocortical network events are temporally linked to hippocampal ripple activity, we first examined average spectrograms of neocortical epochs centered on CA1 ripples. Ripple occurrence was associated with a selective increase of power in the delta and sleep spindle bands (dark red segments in Fig. 1b). The cooccurrence of the respective neocortical and hippocampal events was modulated by slow and ultraslow oscillations at 0.02–0.6 Hz observed previously in the neocortex or hippocampus (Fig. 1b; refs. 12 and 36–39). To quantify this slow time scale temporal relationship between hippocampal and neocortical patterns at the group level, the instantaneous power of hippocampal ripples was correlated with that of neocortical sleep spindles (12–18 Hz) and delta (1–4 Hz) waves. These analyses revealed a robust temporal relationship at the 1- to 2-s time scale in both rats and mice (Fig. 1c and d). Similar relationships were observed in cross-correlograms between hippocampal ripple troughs or CA1 units and neocortical

unit activity (Fig. 1e). These findings confirm and extend previous observations on the rat (23, †).

**Fine Time Scale Analysis.** Cross-correlation of neocortical and CA1 hippocampal units, irrespective of the ongoing network patterns, indicated that neocortical unit activity, on average, precedes hippocampal discharges (Fig. 2a). Subsequent analysis, confined to specific network patterns, revealed that the temporal asymmetry of unit correlation was present during ripples, spindles, and delta waves (Fig. 2b–d). It should be noted that, although for technical reasons we detected delta waves (layer V positive wave of  $\approx 200$  ms, associated with decreased or no unit activity), many of the detected delta waves may formally reflect silent periods of slow oscillations, described in cats and humans (13, 36, 40).

The fine time scale relationship between neocortical and hippocampal activity was investigated further by taking advantage of the established phase-locked discharges of neurons to these respective field patterns. CA1 pyramidal cell discharge is tightly locked to the troughs of hippocampal ripple waves (41), and the troughs of sleep spindles and delta waves in deep cortical

†Battaglia, F. P., Sutherland, G. R. & McNaughton, B. L. (2001) *Soc. Neurosci. Abstr.* 27, 643.16.

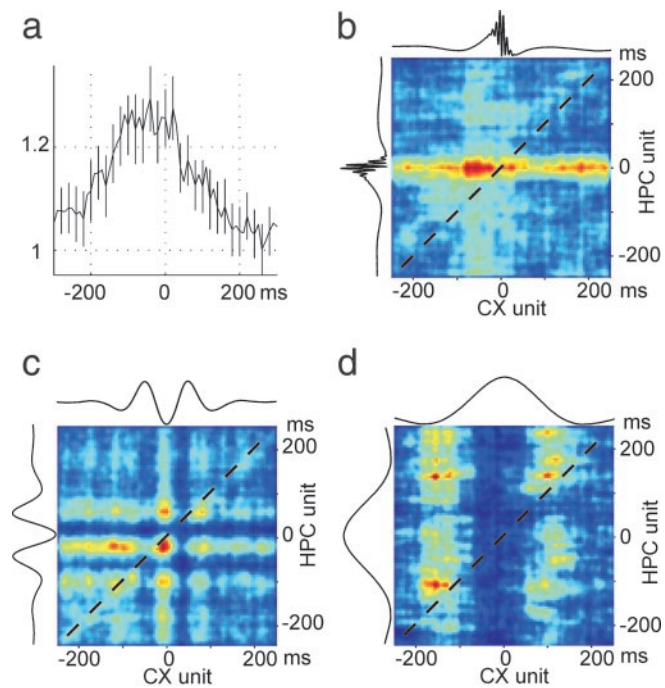


**Fig. 2.** Fine scale temporal relationship between neocortical and hippocampal unit activity during neocortical or hippocampal network events. (a) Cross-correlation between CA1 units (reference) and deep layer neocortical units (mean  $\pm$  SE). Note that neocortical activity precedes hippocampal discharges. (b–d) Joint perievent time histograms of neocortical and hippocampal units referenced to ripple (b), trough of spindle (c), and peak of delta (d). Color scale: joint probability density from low (blue) to high (red) values. Dashed diagonal corresponds to synchronous discharge of neocortical and hippocampal units. Note 50- to 100-ms precedence of neocortical activity during ripple, delta, and spindle events. Data in a are from 10 mice; data in b–d are from a representative mouse.

layers reflect the maximum discharge of neocortical neurons (13). Thus, troughs of field oscillations reflect synchronous discharge of neurons throughout the network, compared with a few locally recorded by the electrode. The peak discharge of hippocampal neurons and the maximum probability of ripple troughs occurred, on average,  $\approx 50$  ms after the troughs of delta waves (Fig. 3a). During neocortical sleep spindles, the peak discharge of hippocampal neurons and the maximum probability of ripple troughs occurred  $\approx 50$  ms after (or  $\approx 20$  ms before, in the 12.5-Hz cycle) the trough of neocortical spindles (Fig. 3b).

**CSD Analysis.** Similar results were obtained in rats ( $n = 4$ ) implanted with multiple-site silicon probes in the neocortex (Fig. 4). We also exploited the advantage of silicon probes and performed CSD analysis to eliminate spurious volume-conducted field potential and to verify cortical origin of spindles and delta waves. Neocortical deep sink-source pairs associated with field spindles and unit activity were accompanied by rhythmic phase-locking of CA1 unit activity (Fig. 4a). A similar relationship was observed during delta waves. The deep-positive peak of delta wave (source in layer V; Fig. 4b) was associated with reduced unit activity in neocortex and hippocampus and increased discharge during the troughs of delta waves in both structures.

Asymmetry of unit–unit cross-correlations and consistent phase-locking of hippocampal activity to the neocortical rhythmic discharges suggested neocortical modulation of hippocampal activity. To explore this possibility, we recorded with multiple-site silicon probes simultaneously in both structures. Neocortical spindles were occasionally associated with rhythmic

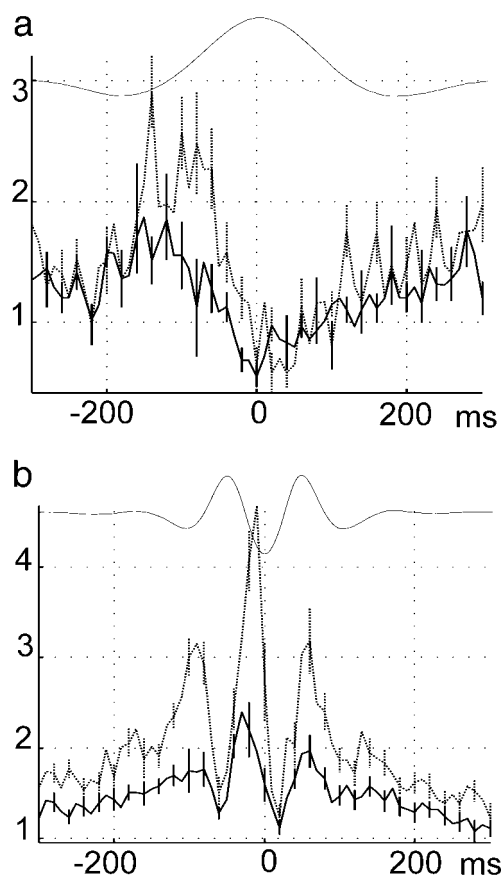


**Fig. 3.** Group data of fine time scale relationship between neocortical and hippocampal activity. (a) Cross-correlogram between delta waves and CA1 hippocampal unit activity (solid) and between delta waves and ripple troughs (dotted; mean  $\pm$  SE). Highest probability of neocortical discharge occurred at the trough of delta waves (not shown). Note peak probability of hippocampal unit activity and ripple occurrence after the trough of delta wave. (b) Cross-correlogram between troughs of sleep spindles and CA1 hippocampal unit activity (mean  $\pm$  SE; solid) and between troughs of sleep spindles and ripple troughs (dotted). Data are from 10 mice. Ordinates: c.i.

sinks in stratum (str.) radiatum of CA3, which were phase-locked to neocortical spindles (Fig. 5). These observations indicate that neocortical activity can reach the hippocampus by way of the entorhinal input. The excitability fluctuations within hippocampal networks, associated with neocortical spindles, could trigger sharp wave-associated ripples in the CA1 region as well (Fig. 5). Cortical delta waves were also associated with a similar depth profile of sinks in the hippocampal CSD (not shown).

### Discussion

Our findings demonstrate that neocortical and hippocampal activity is coupled on both long and short time scales during slow wave sleep. Coactivation of neuronal networks at the suprasecond time scale can be brought about by synchronization of various ultraslow rhythms that these structures are intrinsically endowed with (37–39) and/or by common modulatory drive (42). An important finding of our experiments is the presence of a much finer temporal relationship between neocortical and hippocampal neuronal activity. Superimposed on the ultraslow comodulation of network patterns, neocortical bursts, associated with delta/slow oscillation and spindle rhythms, produced by thalamocortical circuitry (13–15), entrained hippocampal neurons at the 10-ms time scale and triggered population events associated with ripples. On the basis of the latency differences

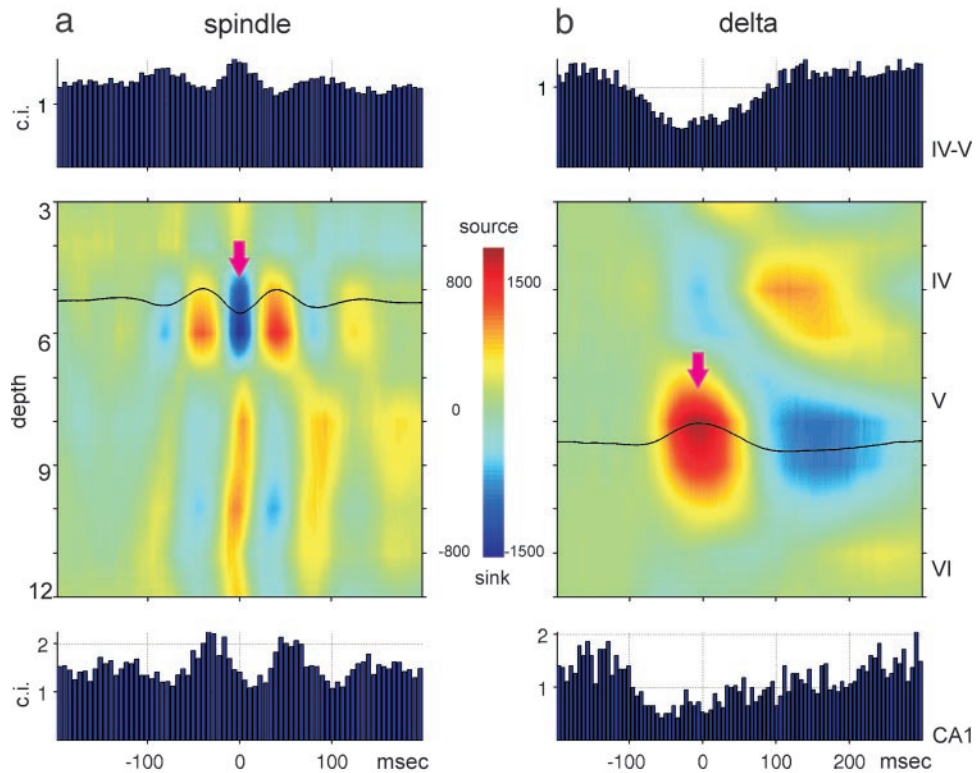


**Fig. 4.** CSD in deep cortical layers related to neocortical and CA1 unit activity in the rat. (a) Averaged neocortical CSD and cross-correlograms between the troughs of neocortical spindles (arrow,  $n = 1,452$ ) and layer IV–V units (Top) as well as hippocampal CA1 units (Bottom). Note phase-locked discharge of neocortical units to spindle troughs and phase-locked and delayed ( $\approx 50$  ms) discharge of CA1 units. (b) Averaged neocortical CSD ( $n = 286$  sweeps) and cross-correlograms between the peaks of neocortical delta waves (arrow) and layer IV–V units (Top) as well as hippocampal CA1 units (Bottom). Note delayed maximal firing of hippocampal neurons. Ordinates: 100- $\mu$ m steps, indicated by recording site numbers (3–12). Approximate positions of neocortical layers are indicated on the right. Multiple unit activity from CA1 pyramidal layer was recorded by site 16 of the silicon probe.

and CSD analyses, it is reasonable to assume that neocortical events activated layer II and III entorhinal neurons (43), which, in turn, induced an excitability bias within the hippocampal networks. Although the emergence of sharp wave bursts does not require extrahippocampal inputs (44), the present findings show that the exact timing of sharp wave bursts can be influenced by neocortical events during sleep.

For formal reasons, we related neocortical delta waves to hippocampal patterns. However, a significant portion of the delta waves was likely part of slow oscillations that are known to modulate neocortical excitability (36, 45). The silence–activity transition of cortical slow oscillation can trigger sleep spindles (13), and the strong population synchrony associated with it could also trigger hippocampal ripples. Within sleep spindles, a fine temporal structure existed between neocortical and hippocampal neurons. The excitability fluctuations of neocortical neurons within the spindle effectively timed ripple occurrence in the hippocampus. In turn, the hippocampal output during ripple likely added further excitation to the next spindle cycle. Alternatively, both neocortical and hippocampal activity can be paced by a common input (e.g., thalamus) during spindles.

The functional importance of the demonstrated coupling between neocortical and hippocampal network activity is that it provides the temporal framework for coordinated information transfer between the two structures. Particularly, we hypothesize that neocortical neuronal discharges, associated with delta wave and spindle events, “select” via the entorhinal input which hippocampal neurons will participate in the triggered ripple events.

Individual sleep spindles emerge from the activity of different thalamic and cortical neuronal assemblies, as evidenced by the variable spatial distribution of spindle power in successive spin-

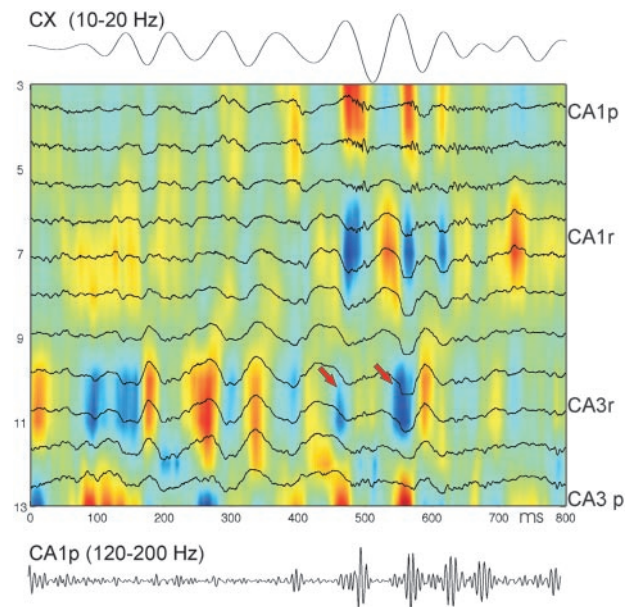


**Fig. 5.** Neocortical spindles modulate hippocampal activity. Shown is a representative example of simultaneously recorded deep cortical electroencephalogram (Top, filtered 10–20 Hz) and CSD map in the hippocampus. (Bottom) Filtered (120–200 Hz) trace from electrode 3 in CA1 pyramidal layer. CA1p and CA3p, pyramidal layer; CA1r and CA3r, str. radiatum. Note that spindle troughs are associated with  $\approx 50$ -ms-delayed sinks in CA3 str. radiatum, some of which are associated with sharp wave/ripple events (arrows).

dle episodes (14). We suggest that these specific inputs can select burst initiators of the hippocampal sharp wave events (46). In turn, the sharp wave/ripple-related discharge of neurons in the CA3-CA1-subiculum-presubiculum-entorhinal cortex axis (21) will provide a synchronous output preferably to those neocortical cell assemblies that continue to participate in the spindle event. Thus, the hippocampal output coexists with the postsynaptic discharge of a specific group of neocortical pyramidal cells, due to the long duration of sleep spindles and/or delta/slow

oscillations. The robust temporal relationship between cortical rhythmic activity and hippocampal ripples suggests that coupling of these network events is an effective mechanism to link neocortical and hippocampal cell assemblies and strengthen their coalition.

We thank Ken Wise and Jamie Hetke for supplying us with the silicon probes (1P41RR09754). This work was supported by National Institutes of Health Grants NS34994, MH 54671, and NS43157.

1. Engel, A. K., Fries, P. & Singer, W. (2001) *Nat. Rev. Neurosci.* **2**, 704–716.
2. Perez-Orive, J., Mazor, O., Turner, G. C., Cassenaer, S., Wilson, R. I. & Laurent, G. (2002) *Science* **297**, 359–365.
3. Marr, D. (1971) *Philos. Trans. R. Soc. London B* **262**, 23–81.
4. Buzsáki, G. (1989) *Neuroscience* **31**, 551–570.
5. Buzsáki, G. (1996) *Cereb. Cortex* **6**, 81–92.
6. Wilson, M. A. & McNaughton, B. L. (1994) *Science* **265**, 676–679.
7. Squire, L. R. (1992) *Psychol. Rev.* **99**, 195–231.
8. McClelland, J. L., McNaughton, B. L. & O'Reilly, R. C. (1995) *Psychol. Rev.* **102**, 419–457.
9. Maquet, P. (2001) *Science* **294**, 1048–1052.
10. Pavlides, C. & Winson, J. (1989) *J. Neurosci.* **9**, 2907–2918.
11. Hirase, H., Leinekugel, X., Czurko, A., Csicsvari, J. & Buzsáki, G. (2001) *Proc. Natl. Acad. Sci. USA* **98**, 9386–9390.
12. Leinekugel, X., Khazipov, R., Cannon, R., Hirase, H., Ben Ari, Y. & Buzsáki, G. (2002) *Science* **296**, 2049–2052.
13. Steriade, M. (2001) *J. Neurophysiol.* **86**, 1–39.
14. Destexhe, A. & Sejnowski, T. (2001) *Thalamocortical Assemblies: How Ion Channels, Single Neurons and Large-Scale Networks Organize Sleep Oscillations* (Oxford Univ. Press, New York).
15. McCormick, D. A. & Bal, T. (1997) *Annu. Rev. Neurosci.* **20**, 185–215.
16. Vanderwolf, C. H. (1969) *Electroencephalogr. Clin. Neurophysiol.* **26**, 407–418.
17. Bland, B. H. (1986) *Prog. Neurobiol.* **26**, 1–54.
18. Buzsáki, G. (2002) *Neuron* **33**, 325–340.
19. Buzsáki, G., Horvath, Z., Urioste, R., Hetke, J. & Wise, K. (1992) *Science* **256**, 1025–1027.
20. Ylinen, A., Bragin, A., Nadasdy, Z., Jando, G., Szabo, I., Sik, A. & Buzsáki, G. (1995) *J. Neurosci.* **15**, 30–46.
21. Chrobak, J. J. & Buzsáki, G. (1996) *J. Neurosci.* **16**, 3056–3066.
22. Connors, B. W. & Amitai, Y. (1997) *Neuron* **18**, 347–349.
23. Siapas, A. G. & Wilson, M. A. (1998) *Neuron* **21**, 1123–1128.
24. Burwell, R. D., Witter, M. P. & Amaral, D. G. (1995) *Hippocampus* **5**, 390–408.
25. Jay, T. M. & Witter, M. P. (1991) *J. Comp. Neurol.* **313**, 574–586.
26. Hormuzdi, S. G., Pais, I., LeBeau, F. E., Towers, S. K., Rozov, A., Buhl, E. H., Whittington, M. A. & Monyer, H. (2001) *Neuron* **31**, 487–495.
27. Csicsvari, J., Hirase, H., Czurko, A., Mamiya, A. & Buzsáki, G. (1999) *J. Neurosci.* **19**, 274–287.
28. Buzsáki, G., Buhl, D., Harris, K. D., Csicsvari, J., Czeh, B. & Morozov, A. (2002) *Neuroscience* **116**, 201–211.
29. Harris, K. D., Henze, D. A., Csicsvari, J., Hirase, H. & Buzsáki, G. (2000) *J. Neurophysiol.* **84**, 401–414.
30. Torrence, C. & Compo, G. P. (1998) *Bull. Am. Meteorol. Soc.* **79**, 61–78.
31. Aertsen, A. M., Gerstein, G. L., Habib, M. K. & Palm, G. (1989) *J. Neurophysiol.* **61**, 900–917.
32. Mitzdorf, U. (1985) *Physiol. Rev.* **65**, 37–100.
33. Freeman, J. A. & Nicholson, C. (1975) *J. Neurophysiol.* **38**, 369–382.
34. Thomson, D. J. (1982) *Proc. IEEE* **70**, 1055–1096.
35. Mitra, P. P. & Pesaran, B. (1999) *Biophys. J.* **76**, 691–708.
36. Steriade, M., Nunez, A. & Amzica, F. (1993) *J. Neurosci.* **13**, 3252–3265.
37. Sanchez-Vives, M. V. & McCormick, D. A. (2000) *Nat. Neurosci.* **3**, 1027–1034.
38. Jando, G., Carpi, D., Kandel, A., Urioste, R., Horvath, Z., Pierre, E., Vadi, D., Vadasz, C. & Buzsáki, G. (1995) *Neuroscience* **64**, 301–317.
39. Zhang, Y., Perez Velazquez, J. L., Tian, G. F., Wu, C. P., Skinner, F. K., Carlen, P. L. & Zhang, L. (1998) *J. Neurosci.* **18**, 9256–9268.
40. Achermann, P. & Borbely, A. A. (1997) *Neuroscience* **81**, 213–222.
41. Csicsvari, J., Hirase, H., Czurko, A., Mamiya, A. & Buzsáki, G. (1999) *J. Neurosci.* **19**, RC20.
42. Golanov, E. V., Yamamoto, S. & Reis, D. J. (1994) *Am. J. Physiol.* **266**, R204–R214.
43. Amaral, D. G. & Witter, M. P. (1989) *Neuroscience* **31**, 571–591.
44. Bragin, A., Jando, G., Nadasdy, Z., van Landeghem, M. & Buzsáki, G. (1995) *J. Neurophysiol.* **73**, 1691–1705.
45. Steriade, M. (1999) in *Electroencephalography: Basic Principles, Clinical Applications and Related Fields*, eds Neidermeyer, E. & Lopes da Silva, F. H. (Williams & Wilkins, Baltimore), pp. 28–62.
46. Csicsvari, J., Hirase, H., Mamiya, A. & Buzsáki, G. (2000) *Neuron* **28**, 585–594.